Domeless Solar Tower Telescope at the Hida Observatory

AUTHOR(S):

Nakai, Yoshihiro; Hattori, Akira

CITATION:

Nakai, Yoshihiro ...[et al]. Domeless Solar Tower Telescope at the Hida Observatory. Memoirs of the Faculty of Science, Kyoto University. Series of physics, astrophysics, geophysics and chemistry 1985, 36(3): 385-399

ISSUE DATE:

1985-03

URL:

http://hdl.handle.net/2433/257590

Memoirs of the Faculty of Science, Kyoto University, Series of Physics, Astrophysics, Geophysics and Chemistry, Vol. XXXVI, No. 3, Article 1, 1985

Domeless Solar Tower Telescope at the Hida Observatory*

By

Yoshihiro NAKAI and Akira HATTORI**

Kwasan and Hida Observatories, Yamashina, Kyoto 607, Japan

(*Received January 26, 1983*)

Abstract

Domeless Solar Tower Telescope was designed, assembled and built at the Hida Observatory successfully. This system includes Gregory-telescope, vertical spectrograph, horizontal spectrograph and auxiliary instruments such as cooling panels around the tower. The achieved best resolusion of the solar image is 0.3″.

Keywords: Solar telescope, Local seeing, Spectrograph, Control system.

1. Introduction

In the fall of 1968, the Tsugami 60-cm reflector of the Kwasan Observatory was removed to the Hida Observatory, which is a new station decided after two years' site survey to escape from increasing city lights and contamination. As a next project of the observatories' extending program, a new solar telescope to get the details as fine as possible was considered. With the secured experience on solar observation with the solar telescope at the Kwasan Observatory (Nakai and Kubota 1963), our recognition that the instrument for modern solar observation should produce high resolution image of 0.5″ first and should be complemented by a high dispersion spectrograph of 0.1 Å/mm was fixed.

During the time, from 1962 to 1974, some solar telescopes were built at Sydney (Loughhead et al. 1968), Sacramento Peak (Dunn 1969), Kitt Peak (Pierce 1969), Big Bear (Zirin 1969) and so on, and these have produced epoch-making high resolution photographs of the sun, which were resulted by newly-devised design come from the comprehensive studies of seeing condition mainly.

In our design policy, to minimize the image defects due to local seeing caused by solar radiation and by wind, the dome, which is an origin of turbulences, should be eliminated. We should put the telescope up to about 20 m high on the tower in order to put the entrance-window into laminar air flow where effects of local convection from the heated ground would be reduced. The concrete tower in sunshine is another source of convection, also. Then its surface should be covered with stainless panels, whose surface-temperatures should be controlled within nearly as same temperature as that of the surrounding air. There is another problem

*) Contributions from the Kwasan and Hida Observatories, No. 260.

**) deceased on Jan. 23, 1983 by sudden apoplexy stroke.

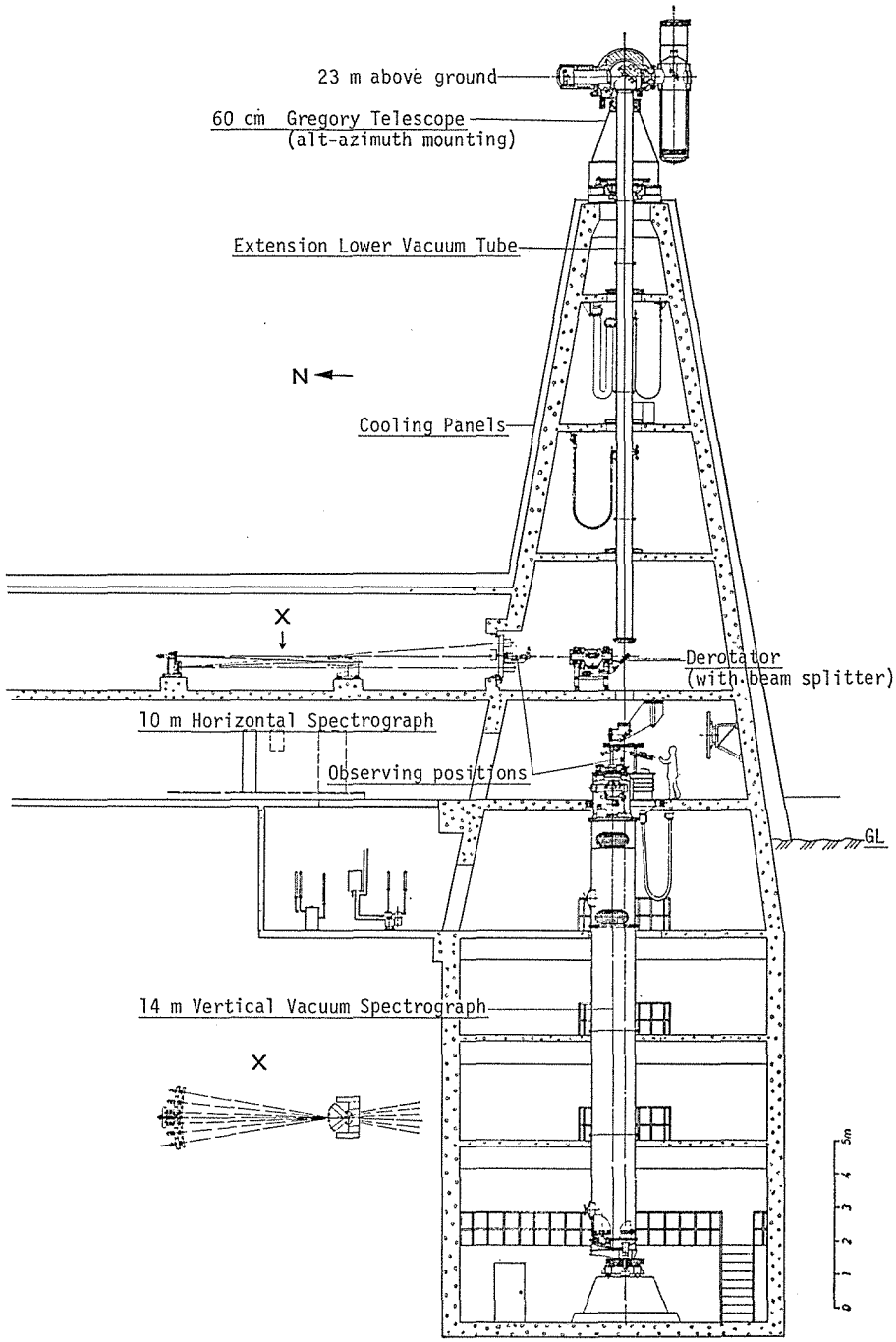

Fig. 1. Domeless Solar Tower Telescope consists of Gregory-telescope, vertical vacuum spectrograph and horizontal spectrograph.

of the tower-stability. Vibrations and twist-motions of the concrete tower, on which 24 tons telescope should be supported, is analyzed and the results show that 50 cm thickness of the reinforced concrete wall would be stiff enough to be stable within an accuracy of 0.2″ in both altitude and azimuth directions against the wind of 10 m per sec.

For the purpose of spatially wide spectroscopy, two types of dispersion, should be necessary: high dispersion spectrograph and medium dispersion spectrograph of wide spectral range.

For the former, 14 m vacuum vertical spectrograph is planned. In addition to the usual 50 mm height slit, 150 mm height curved slit should be equipped for spectroheliographic observation. Because of the required wide field, total system of vertical vacuum spectrograph should be rotatable to compensate image rotation without use of a derotator.

For the latter, Czerny-Turner system of 50 mm height slit is adopted instead of an Echelle system. Because, our requirement is to obtain solar spectrum not only in the wide spatial field but in wide spectral range. To cover wide spectral range simultaneously, six camera mirrors and corresponding six cameras are adopted. A derotator with three mirrors can be put in front of the fixed slit. Figure 1 shows a schematic drawing of the telescope, spectrographs and building.

2. Local Seeing

For the solar observation, image qualities are affected by refractive inhomogeneities in the lower atmosphere which would be caused by the convection from the heated ground and by wind as well as in the upper atmosphere. Especially, fluctuation in the refractive index of the air —that is proportional to the thermal fluctuation in the air— is dominant in the plume rising from the heated ground due to the solar radiation, but is rather quiet outside the plume. This characteristic is significant when height increases, because such turbulence is mainly due to mechanical turbulence when the wind shears off the heated bubble from the ground. In accordance with the shape and motion of the plume, which is shown in figure 3, it is clear that the blurring effect of the refractive inhomogeneities on the solar image is significant at lower height. An optimized height of the telescope should be decided after observing the thermal fluctuation at several heights as a point where the duration of quiet time is reasonably long at a height accessible to us. For this purpose, some experiment similar to Lynds (1962) are carried on the observatory ground (Mitsuda 1977). Before that time, preliminary experiments to see the flows of air over the prcposed sites with smoke-screen stacked up to 20 m high were done, and two points are proposed already. Temperatures at 8, 13, 18, 23 and 28 m high are measured with high speed thermal sensors and with the multichannel data recorder. At 23 m high, the relative humidity and wind velocity are measured simultaneously. Figure 2 shows a portion of thermal record of temperature variation played back to a pen recorder. Quiet regions, marked as T.Q., clearly become longer in proportion as an observing point is higher. Figure 3 shows typical figure

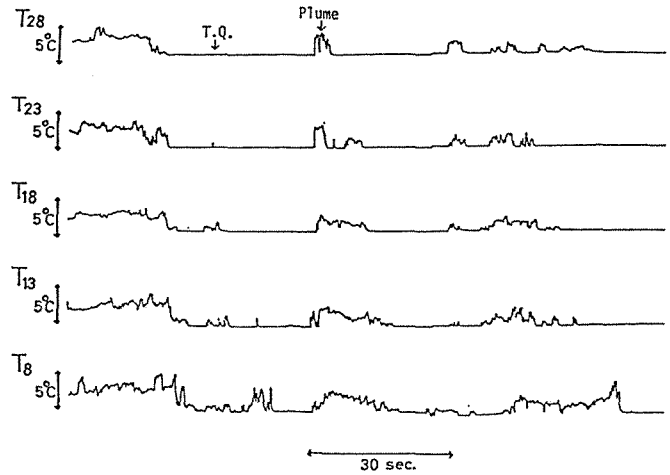

Fig. 2. Temperature fluctuation at 8, 13, 18, 23 and 28 m high respectively. Time increase left to right. (After Mitsuda)

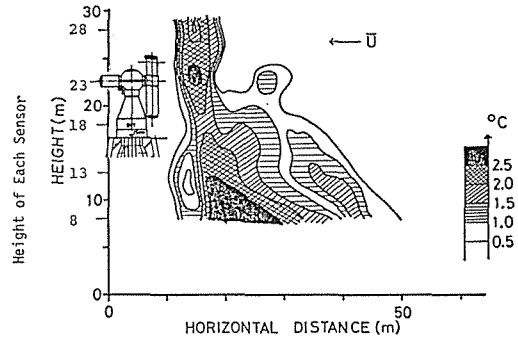

Fig. 3. Typical figure of a PLUME taken at the site No. 2. Horizontal distance is estimated from wind velocity $\bar{U}$ and duration time. Actual position of the telescope is shown. (After Mitsuda)

of a plume occurred at the site No. 2. At the upper left corner in this figure, the actual position of the telescope is shown.

Probabilities of duration time from 0 to 10 sec are calculated from morning to evening. We define as quiet region where the temperature fluctuation is less than 0.05°C. Figure 4 shows the results.

Nothing to say, a higher position should be much suitable for our purpose, but except for the case of evening, no significant difference can be seen between the two curves of 28 and 23 m high. So, we decided to put the entrance-window at higher than 23 m above the ground level.

Another turbulence would rise from the tower itself. Concrete surfaces in sunshine are heated and get warming up to higher than 50°C. These would excite new turbulences neighbouring to the entracne-window. Without eliminating such type of disturbance, our purposes for building the tower to reduce turbulences from the ground could not be accomplished.

In order to reduce this disturbance, 1) passively, concrete surface should be covered with high reflective stainless-steel-plates or coated with titan-white (TiO_2) paint, and 2) positively temperature of the surface should be kept as same as the

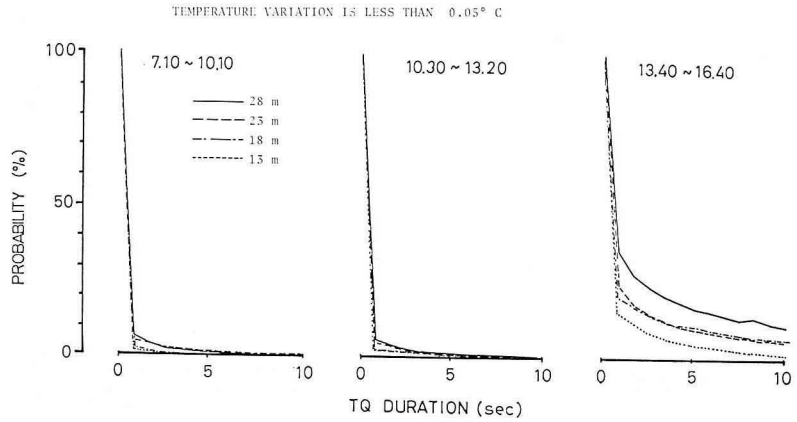

Fig. 4. Probability of duration time from 0 to 10 sec is calculated at each height from morning to evening. Percentage values of morning, noon and afternoon are shown from the left to right. Here, as for the thermal quiet region, we defined the region where temperature variation is less than 0.05°C.

Fig. 5. General view of the Domeless Solar Tower Telescope to the East. The tower is covered with temperature controlled stainless panels. Besides the upper six stages, buildings are covered with mere stainless steel plates. Neighboring building and passage-way are coated with titan-white paint.

air temperature surrounding the tower. Therefore, the tower should be fully covered with cooling panels as is shown in figure 5. In the figure 6, a typical record of the temperature of each panel-section around the tower is shown. Figure 7 is

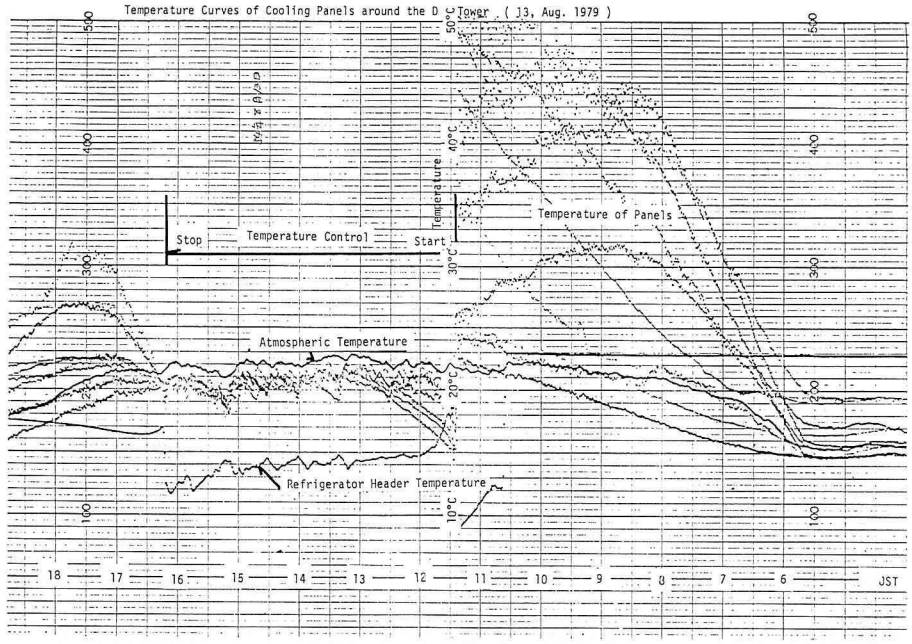

Fig. 6. This record shows temperature variation of each section of cooling panels around the concrete tower and of the atmospheric temperature. 5:30 a.m.; after sunrise, temperature goes up gradually, 11:30 a.m.; circulation of cooled water into the water-jackets behind the panels starts, and after few minutes their temperature goes down below the atmospheric temperature. Some of the panel-planes become over-cooled once, but soon all of them are settled within $+0°C$ and $-3°C$, by the function of servo-controllers equipped individually.

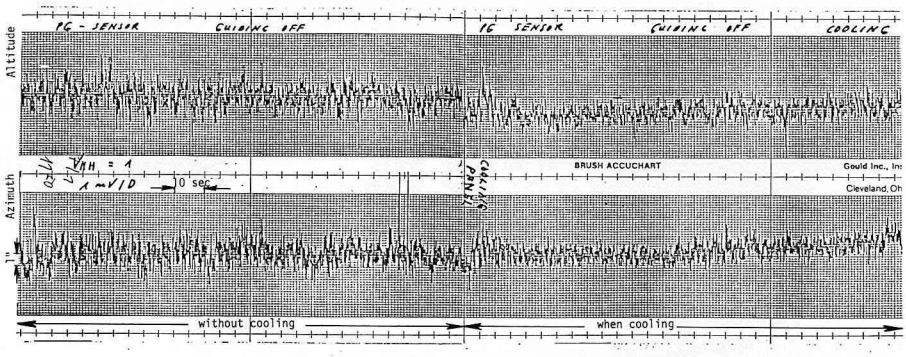

Fig. 7. Two traces were taken during the test of the telescope tracking. Signals came from Reticon sensors put on the limb of the primary solar image. Pen deflection is proportional to the shift of solar limb. Shift consists of slowly changing tracking error and high frequency seeing noise. Upper trace is of altitude component, and lower one is of azimuth component. Left half records shows seeing noise without cooling and right hand when cooled. Time scale is 1 second/minimum division and seeing scale is 1″/5 divisions. Cooling effects to reduce amplitude of seeing.

a portion of records of tracking error test of the driving. Signals are taken from two Reticon sensors radially put on the limb of the primary image of the sun. Upper trace is of the elevation component and lower one is of the azimuthal. Left half is a record without cooling and right hand is with cooling. Improvements in reducing the amplitude and in eliminating sharp spike-like-pulses due to cooling the tower can be seen.

3. Gregory Telescope

The telescope is of alt-azimuth mounted Newton-Gregory configurations. As shown in figure 8, solar ray enters the BK 7 entrance-window with a free aperture of 605 mm and thickness of 40 mm. Around free aperture, the edge of the window is covered with aluminized mosaic quartz-mirrors in order to avoid the heat concentration on the edge of the window which results in the deformation of window (Kühne 1978). Then ray goes through an entrance pupil with an aperture of 600

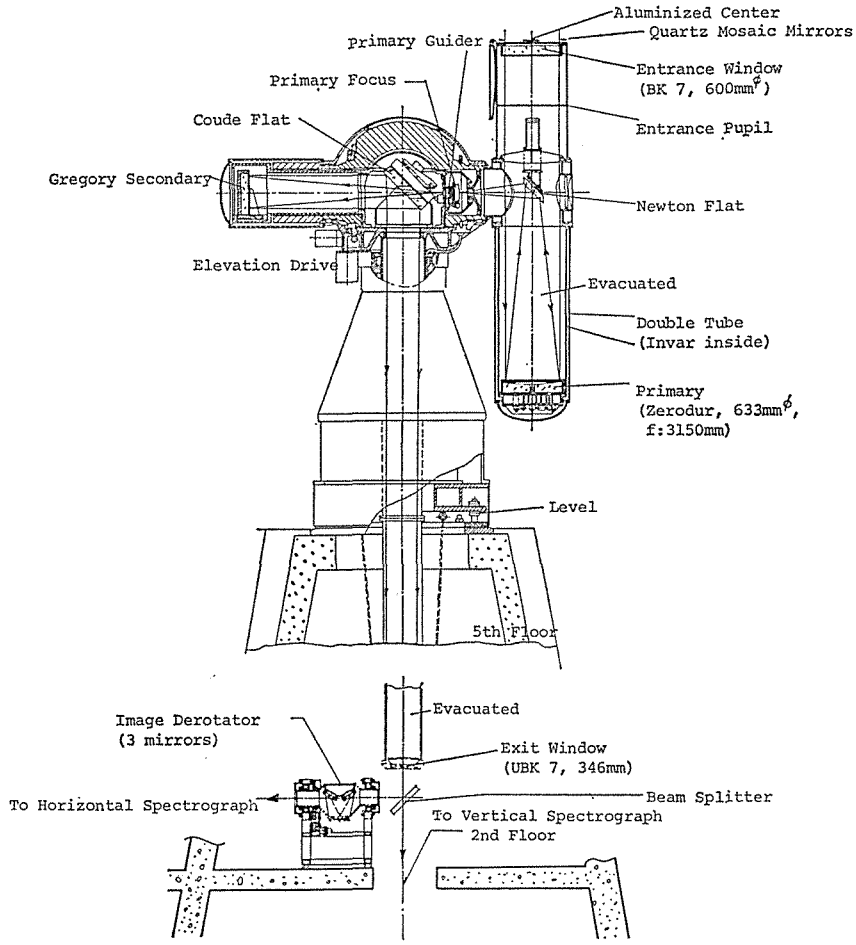

Fig. 8. Schematic drawing of the Gregory-telescope.

mm until it strikes primary mirror of 633 mm in diameter. The primary is made of Zerodur and its cell is supported by Invar inside-tube in order to fix the primary image on the focal plane defined mechanically, where one of the occulting cones or diaphragms is put in. All other mirrors are also made of Zerodur and free from thermal distortion of optics. The primary has a focal length of 3150 mm and forms solar image of about 30 mm in diameter on one end of elevation axis of the tube, where a primary guider and a turret of occulting cones and diaphragms are located. By insertion of occulting cone of suitable size for the observation at the solar limb, and by insertion of diaphragm of selected size for the object on the solar disk, superfluous light can be reflected and the greater part of the stray light is eliminated. All of them are cooled with refrigerated water flow. Light goes further through a central hole of Coude mirror until it strikes the Gregory secondary mirror of 452 mm in diameter. The composite focal length is 32, 190 mm and the *f*-ratio is 53.7. The Gregory mirror forms a solar image of about 30 cm in diameter at the observing table on the first floor of the solar building. About 88% of total space of light path, i.e., 28 m, from the entrance-window to the exit-window is kept vacua down to 2 mmHg by suction. Deformation due to pressure difference at the windows amounts to 90 μm at the center, which results in defocussing of 0.07 mm that corresponds wave-front error of $\lambda/100$ which is still negligible. Total wave-front errors at the secondary image is $\lambda/16$ (r.m.s.). Linear obscuration by the Newton flat mirror and its mountings is 0.39. Effective image field is 36′.

4. Vertical Vacuum Spectrograph

For high dispersion spectrograph, we planned 14 m vertical vacuum spectrograph. Such a long focal length as 14 meters, which is usually limited by *f*-ratio and by grating ruled area, was decided according to the circumstances that several kinds of grating with ruled area of 306×408 mm^2 is easily obtained commercially (Löwen 1972). Czerny-Turnar type optics are enclosed in a 12 m^3 vacuum tube. Its optical configurations are shown in figure 9. Light passes through a UBK 7 mirror-slit whose back side is figured in a field lens, and through stacked filters which work as order-sorter, and through UBK 7 entrance-window, whose upper surface is shaped as a weak negative cylindrical lens. Then light goes down until it strikes the collimator mirror of 405×282 mm^2. The collimator sends the parallel light-beam of 261 mm in diameter to the reflection grating and illuminates it uniformly. The camera mirror of 532×405 mm^2 images a solar spectrum on the focal plane through UBK 7 plane-parallel exit window. Maximum format size of spectrum is 50×250 mm^2. By the adaption of cylindrical lens as the entrance-window instead of adaption of off-axis parabolae to camera mirror and collimator some amount of astigmatism is reduced. As seen in figure 10, although asymmetry of distribution still remains, spot-diagrams at the utmost edge of the format show that astigmatism, i.e., a diameter of circle of least confusion, is less than 22 μm. By the way, astigmatism without a cylindrical lens is 63 μm and with off-axis parabolae is 36 μm. The adopted maximum slit height is 50 mm, but this spectrograph can serve as a

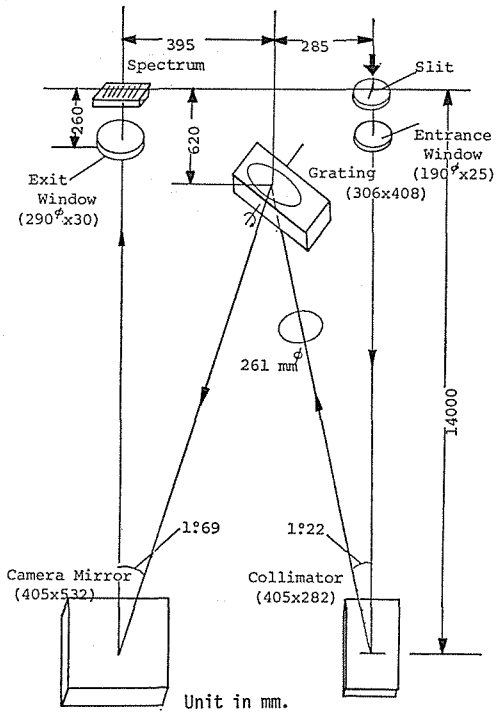

Fig. 9. Schematic drawing of the vertical spectrograph.

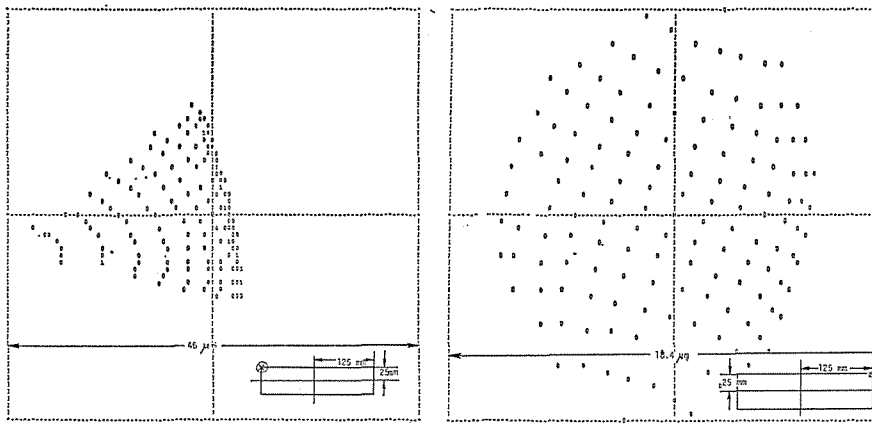

Fig. 10. Spot-diagram calculated to the vertical spectrograph with the entrance-window shaped in weak cylindrical lens. Left hand diagram is of upper-left hand edge of format (250×50 mm^2) and right hand one is of upper-right hand edge of format. Frame size is, from left to right, 46 μm and 18 μm respectively.

heliograph where 150 mm height curved slit is used. Figure 11 shows reciprocal dispersion and grating angle for two type gratings adopted.

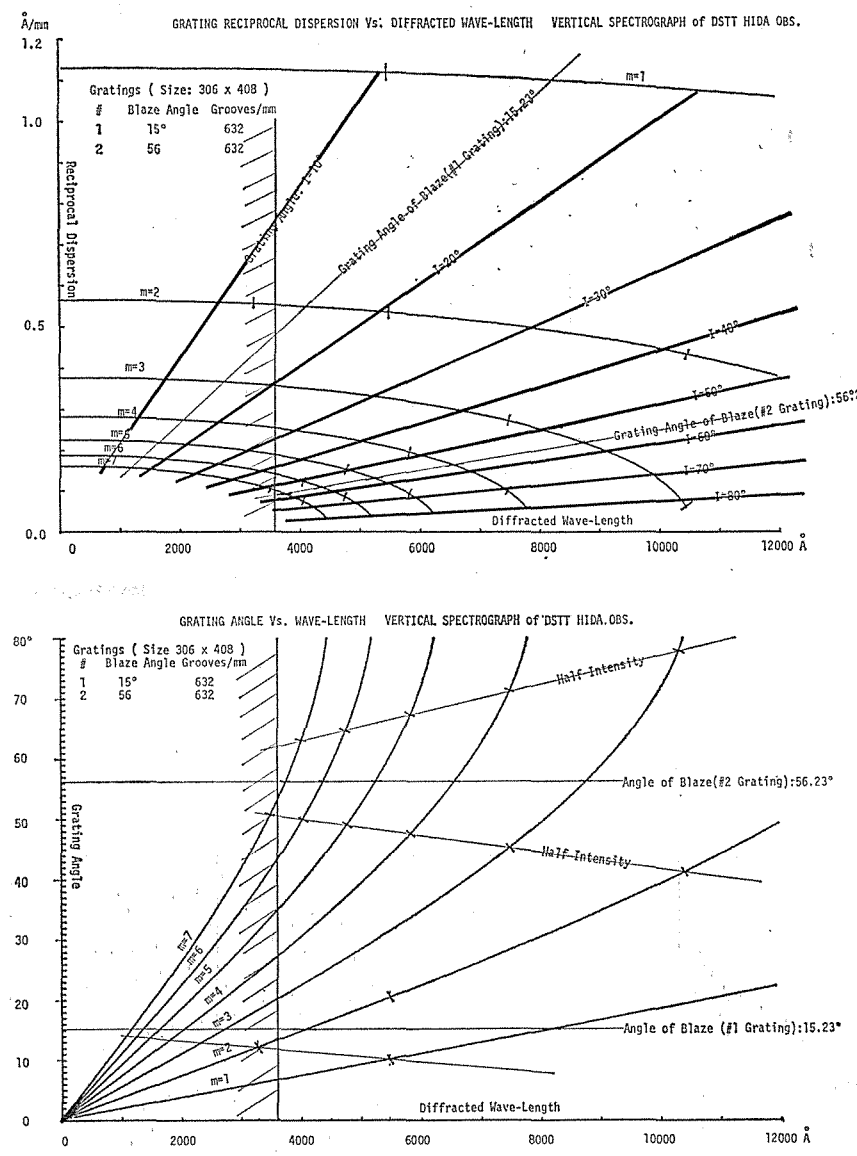

Fig. 11. The vertical vacuum spectrograph is equipped with two gratings of 306×408 mm^2 ruled area and of 632 grooves/mm. Blaze angle is 15° and 56°, respectively. Upper shows reciprocal dispersion and wave length. Lower shows grating angle and wave length.

5. Horizontal Spectrograph

A horizontal spectrograph is accompanied as a complemental instrument to the vertical spectrograph. A 10 m spectrograph is of Czerny-Turnar configurations of off-plane where a grating is installed at a position of $0.45 \times$ focal-length. Figure 12 shows its configuration. Light that is limited in a linear size less than 60 mm

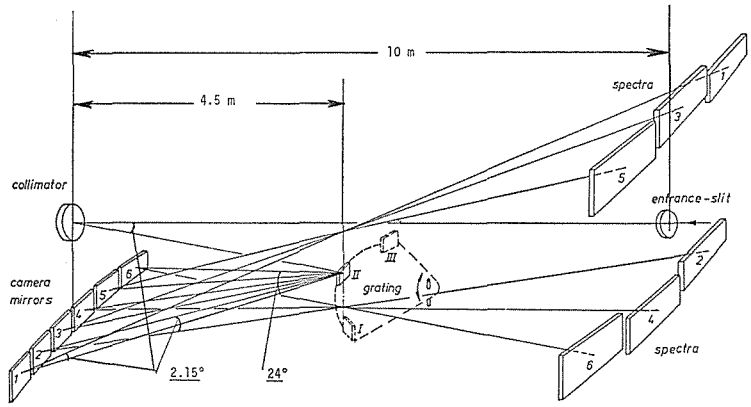

Fig. 12. Optical configuration of the horizontal spectrograph. This system is equipped with three gratings of 150×200 mm² ruled area, remotely interchangeable each other. Six camera mirrors correspond with six camera ports each other.

at slit, with diaphragm at the prime focus, is reflected by a beam splitter (see figure 8) to the slit through a image-derotator, and goes through slit and filters stacked until it strikes a collimator mirror of 215 mm in diameter. Total focal length of this collimator is 10 m. This collimator sends parallel beam to a selected one of three gratings installed in a grating turret. The size of ruled area is 154×206 mm². Diffracted light spreads over six camera-mirrors, each of which forms solar spectrum on corresponding camera port of 70 cm wide. For a wide spectral range observation, when #1 grating is used (Blaze angle: 17°27′, Grooves/mm: 1200), for example, solar spectrum from 3300 Å to 6900 Å is formed on six ports in succession

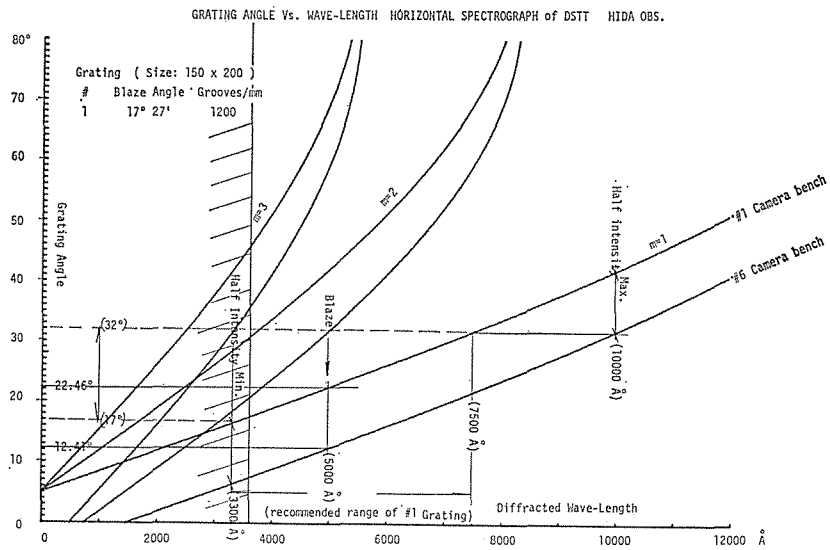

Fig. 13. This diagram shows grating angle and diffracted wave length at the center of No. 1 and No. 6 camera ports of the horizontal spectrograph. Spectral range between them can be photographed at No. 2, No. 5 camera ports, simultaneously.

with small five gaps between camera mirrors. Because of the limited width of camera format of only 240 mm in width, we get discrete spectra due to mechanical restriction. However, in order to take picture at the actual interesting spectral ranges, selection of observing mode such as dispersion, grating, its order, grating angle and positions of camera on ports are practically achieved more easily than expected in planning stage. And, spatially wide field with 50 mm height slit and wide spectral range above-stated are more powerful than using ordinally Echelle spectrograph. Figure 13 shows spectral range which can be photographed simultaneously.

6. Control

Systems are controlled by the DEC PDP-11/45 computer, which has 32 KW main core memory and dual drives of RK05 disks. Control data are transferred to the instruments in DMA mode, in 20 Hz for control operations and in 4 Hz for computations and data displays. Calculations of R.A., Dec., solar diameter, alta-

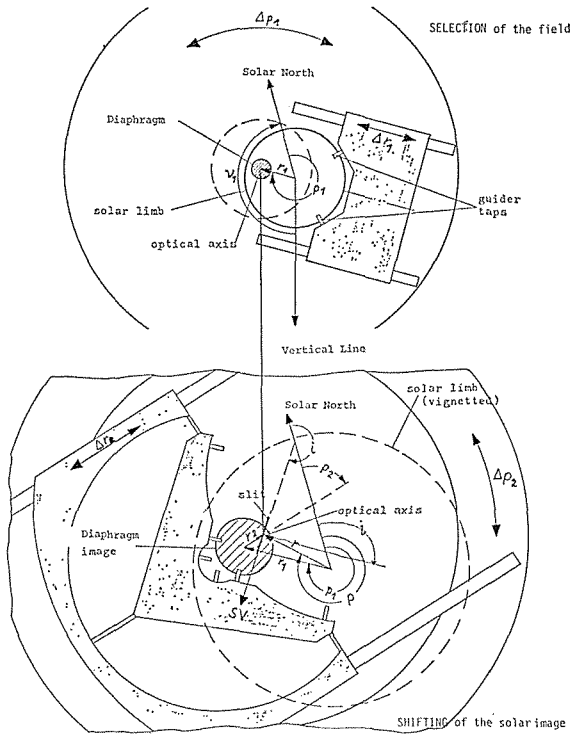

Fig. 14. Taps of PG- and SG-guiders are moved in both direction of polar coordinates around the main axis, respectively. Upper: shifting the PG, limb of the solar image follows to the moving of its coordinates change to (r_1, p_1). In this case, diaphragm is used. Lower: taps of SG-guider corresponding to the diameter of diaphragm catch the limb of the image of diaphragm. Shifting SG, its coordinates change to (r_2, p_2). Polar sum shows (r, p).

zimuth coordinates, atmospheric refraction and others are made one fourth sec. and data are refreshed in 4 Hz. The computer gathers positional information from absolute encoder at each axis and calculates necessary data, and then transfers them to each axis to control speed. Three guiders are equipped with the telescope, i.e., a primary guider neighboring the prime focus, and two secondary guiders, one at the top of the vertical spectrograph and another at the front of the horizontal spectrograph respectively. Error signal from the primary guider compensate position of the telescope itself, and signal from the latter, moves the Coudé mirror to set up the image position. By changing the position of both guiders remotely, the solar image can be also shifted along with their radial and tangential motions. A guider consists of two sensors put apart 90° around the solar limb and can be set in the directions of polar coordinates or altazimuth coordinates at will. Therefore we can select positions in polar coordinates as well as Cartesian coordinates and read off the position data referred to center of the sun on display panel. Figure 14 shows function of the motion of the taps, i.e., diode-array sensors, of the guider and the image position. By shift of one pair of taps of the PG-guider, which usually catches the solar limb and can be moved in two directions of polar coordinates centered at the main optical axis, the solar image follows the moving of PG-guider from previous (0, 0) to (r_1, p_1). As is shown in figure 14-(a), a diaphragm can be introduced at the center. Figure 14-(b) shows similar mechanism of SG-guider. In this case, corresponding pair of taps catches the limb of the image of diaphragm. With shifting of SG-guider, center of the diaphragm moves to the point (r_2, p_2). Then, coordinates of the solar image at the slit-center are of the polar sum (r, p). The observational mode such as sequential shift of image can be done automatically. The most important for astronomers is not the system configurations but the simplicities in handling. During the observation, interfaces between solar astronomers and the telescope are only push-buttons and digital switches in our case.

7. Concluding Remarks

Manufacturing of the telescope started at Carl Zeiss, Oberkochen, Federal Republic of Germany, at 1975, and at the beginning of 1978, it was delivered to Hida observatory. From August of the same year, assembling works are carried on. After nine monthes' effort the telescope system, buildings and their auxiliary equipments are roughly assembled and adjusted. During the same period, control software is developed. On 7th Dec., 1978, first light was introduced to the system, and then on 26th May, 1979, inauguration of Domeless Solar Tower Telescope was held.

Test observations, combined with debugging the software and examining the hardware, proceeded to get fine details of the solar atmospheric structures through the Hα filter. An Hα photograph taken on 14th Aug., 1979 shows fine details of moustaches, which can be resolved up to 0.5″. In July 1980, average seeing condition of about 1″ lasted for two hours, and phenomena of active regions were analyzed with cinematographic techniques (Kawaguchi et al. 1982). After April 1981,

machinetime is opened to solar astronomers outside our Observatories. An electronic data acquisition system, SIT-TV, is beeing tested at the focus of the vertical spectrograph to see the feasibilities in place of photography, and systems of a cinecamera, a high-speed densitometer with image analyzer are now under developing.

Finally to say, ten years and three thousand million yens are spent to build a Domeless Solar Tower Telescope system. We believe that this instrument could make best solar observation in Japan, also is comparable to others built at the best seeing sites over the world. Figure 15 shows an Hα photograph taken on 24th July 1981. The spatial resolution would be better than 0.3″, and is nearly limit of optical resolution. Good seeing conditions and high quality optics would be a powerful instrument in the field of solar physics.

References

Dunn, R.B. 1969, Sky Telesc, **38**, 368.
Kawaguchi, I. et al. 1982, Solar Phys. **78**, 101.
Kühne, C. 1978, in Proc. of the JOSO workshop, held at Firenze, eds. G. Godoli, G. Noci and A. Righini (Tip. Baccini & Chiappi Firenze) p. 57.
Löwen, E.G. 1972, in Proc. of ESO/CERN conference on auxiliary instrumentation for large telescope, held at Geneva, eds. S. Laustsen and A. Reiz (ESO/CERN, München) p. 193.
Loughhead, R.E. 1968, Solar Phys. **4**, 185.
Lynds, C.R. 1962, in IAU Symp. No. 19, held at Rome, eds. J. Rösch, G. Courtes and J. Dommanget (Reidel, Dordrecht) p. 126.
Mitsuda, Y. 1977, in a limited edition, Weather research report accompanied with Domeless solar tower telescope project of the Hida Observatory, (in Japanese).
Nakai, Y. and Kubota, J. 1964, Mem. Coll. Sci. Kyoto Univ., **30**, 323 =Contr. Kwasan Obs. Kyoto, No. 131.
Pierce, A.K. 1969, Solar Phys. **6**, 498.
Zirin, H. 1969, Sky Telesc, **51**, 215.

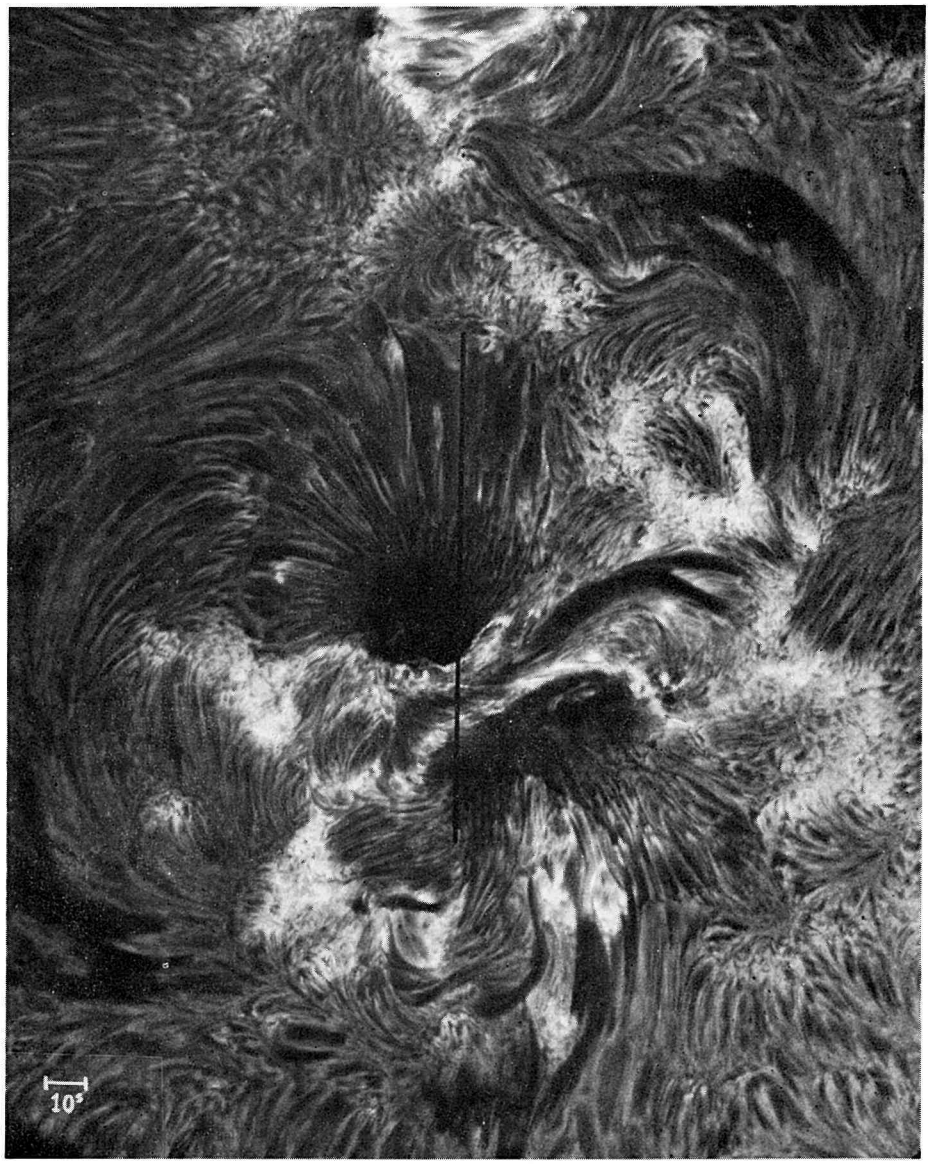

Fig. 15. Hα photograph taken on 24th July, 1981. Bandwidth is 0.25 Å at Hα center, and spatial resolution is better than 0.3″, referring to the slit width of 1″.